Electronic Supplementary Material (ESI) for Journal of Materials Chemistry C.

Supporting information for:

Electrochemically deposited interlayer between PEDOT:PSS and phosphorescent emitting layer for multilayer solution-processed phosphorescent OLEDs

Tiancheng Yu,[a] Jin Xu,[a] Linlin Liu*,[a] Zhongjie Ren*,[b] Wei Yang,[a] Shouke Yan,[b] and Yuguang Ma[a]

[a]Institute of Polymer Optoelectronic Materials and Devices, State Key Laboratory of Luminescent Materials and Devices, South China University of Technology, Guangzhou 510640, P. R. China

[b]State Key Laboratory of Chemical Resource Engineering, Beijing University of Chemical Technology, Beijing 100029, China.

msliull@scut.edu.cn; renzj@mail.buct.edu.cn

Table of Contents:

1. The CV curves of ITO, ITO/PEDOT:PSS and ITO/PEDOT:PSS/SimCP2

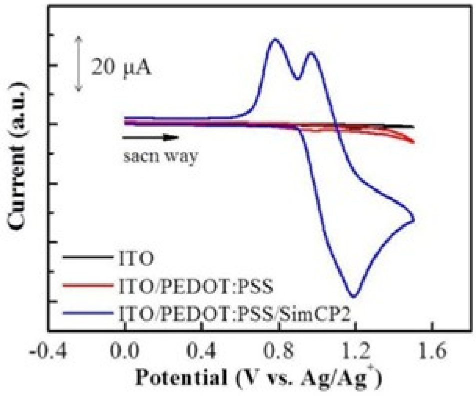

Figure S1. The CV curves of ITO, ITO/PEDOT:PSS and ITO/PEDOT:PSS/SimCP2 under the same conditions: 0.1 M $TBAPF_6$, scanning potential region: 0 to 1.5 V, solvent mixture: V_{CH3CN}/V_{CH2Cl2} = 3 : 2, and scanning rate: 0.05 V s^{-1}.

2. Absorption spectrum of ECP thin film before and after rinsing

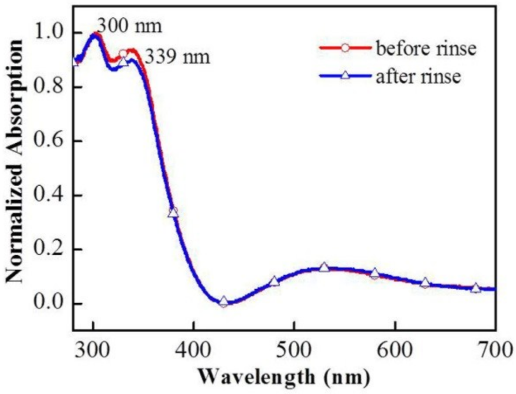

Figure S2. Absorption spectrum of ECP thin film on ITO/PEDOT:PSS substrate before and after rinsing with *p*-xylene.

3. FT-IR spectra of the SimCP2 powder and its ECP film

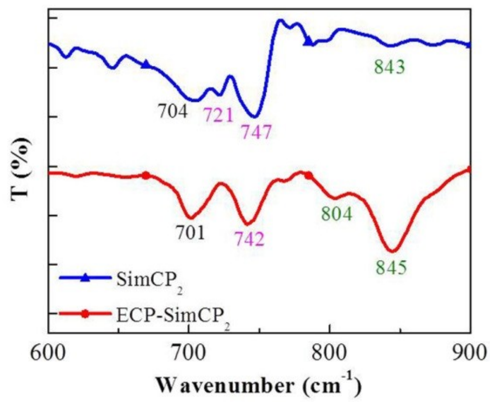

Figure S3. FT-IR spectra of the SimCP2 powder and its ECP film prepared by potentiostatic potential mode at 1.04 V.

The FT-IR spectrum of SimCP2 powder and its electropolymerization film prepared by potentiostatic potential mode at 1.04 V were carried out to examine the cross-linked structure of ECP film. As shown in Fig. 2, the peak at 701 cm^{-1} in ECP film (and 704 cm^{-1} in monomer sample) is attributed to the vibrational bands of C-H bonds of mono-substituted benzene ring, the peaks at 721 cm^{-1} and 747 cm^{-1} in monomer sample (and 742 cm^{-1} in ECP film) are attributed to the bisubstituted benzene ring in carbazole ring. The peak at 843 cm^{-1} in SimCP2 powder is assigned to the trisubstituted phenyl ring while a newly generated peak at 804 cm^{-1} and the peak at 845 cm^{-1} in ECP film are attributed to the trisubstituted phenyl ring in dimeric carbazole unit. The intensity reduction of bisubstituted benzene ring at 747 cm^{-1} and the intensity enhancement of trisubstituted phenyl ring at 845 cm^{-1} as well as a new peak at 804 cm^{-1} indicate the coupling reactions occur among the monomers.

4. The molecular structure of light-emitting material

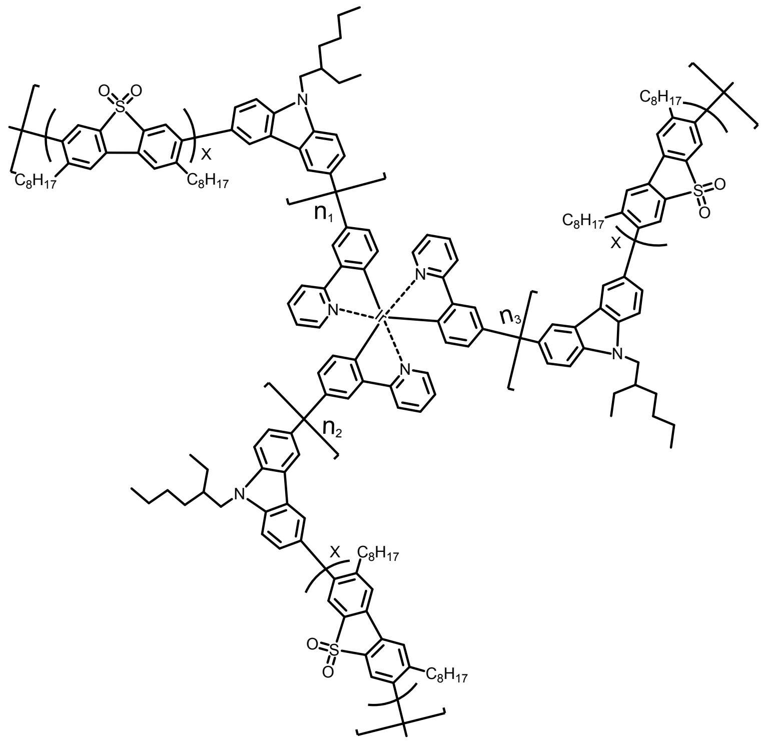

Figure S4. The molecular structure of light-emitting material HBIr.

5. Optical properties of the EML without and with ECP interlayer

Table S1. Optical properties of the EML without and with ECP interlayer of 18 nm

Sample	PLQY
ITO/PEDOT:PSS (40 nm)/EML (45 nm)	7.7%
ITO/PEDOT:PSS (40 nm)/ECP interlayer (18 nm)/EML (45 nm)	14.1%

6. The EL spectra of PhOLEDs devices with ECP thin layer of different thickness.

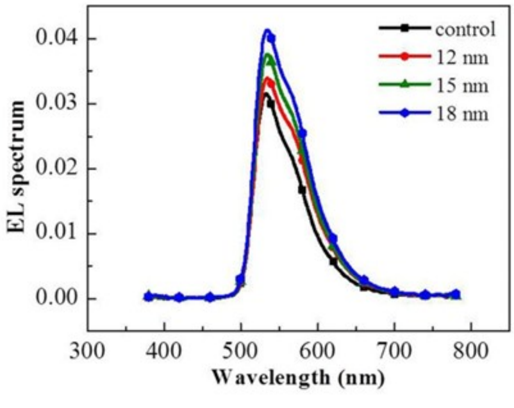

Figure S5. The EL spectra of PhOLEDs devices with ECP thin layer of different thickness at 2mA

7. The PL spectrum of ECP thin film at low temperature

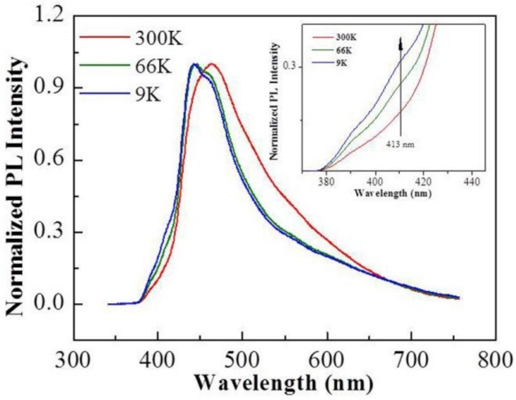

Figure S6. The PL spectrum of ECP thin film at low temperature.

8. CV measurement for the HOMO level of ECP film based on SimCP2

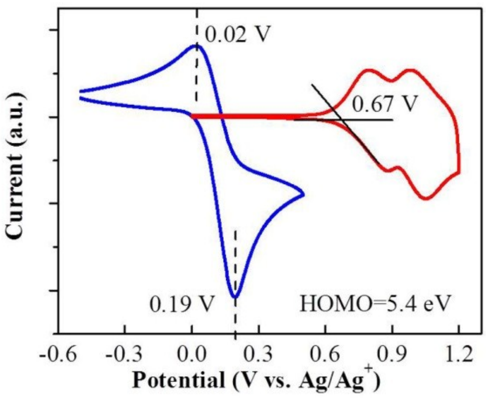

Figure S7. CV curves of ECP film based on SimCP2 (red line) and ferrocene (blue line) under conditions such as: 0.1 M $TBAPF_6$, solvent mixture: CH_3CN and scanning rate: 0.05 V s^{-1}.

9. Impedance Spectroscopy of the PhOLEDs without and with ECP interlayer

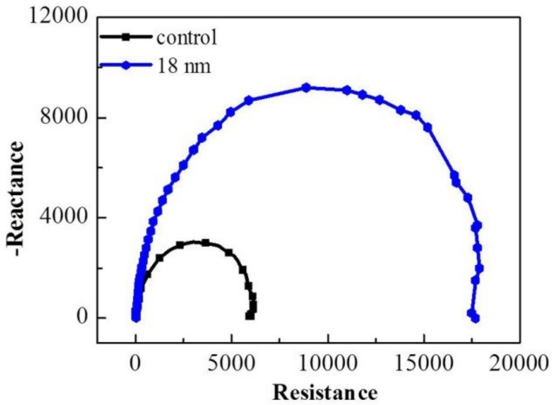

Figure S8. Impedance spectroscopy of the PhOLEDs without and with ECP interlayer of 18 nm.

10. The normalized EL spectra of PhOLEDs devices with ECP thin layer of different thickness

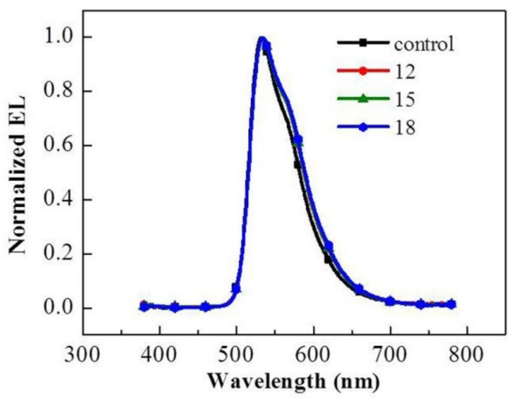

Figure S9. The EL spectra of PhOLEDs devices with ECP thin layer of different thickness.